International Journal of Advanced Technology and Engineering Exploration, Vol 10(101)
ISSN (Print): 2394-5443 ISSN (Online): 2394-7454
http://dx.doi.org/10.19101/IJATEE.2022.10100553

Research Article

Analysis and modelling of the rotor dynamics of a composite hollow shaft using finite element techniques

Ala'a Al-Falahat*
Department of Mechanical Engineering, Mutah University, Mutah, Al-Karak 61710, Jordan, P.O. Box 7

Received: 17-December-2022; Revised: 11-April-2023; Accepted: 14-April-2023

Abstract
A shaft is a crucial component of a rotating machine that transfers energy from its source to the necessary part. In the past two decades, composite materials have been extensively investigated and utilized for rotating shafts due to their relatively high modulus and specific strength without compromising the component's dependability. Carbon/epoxy and boron/epoxy composite materials are often employed and compared to conventional steel shafts. In this study, a finite element analysis tool, engineering simulation software (ANSYS) was utilized for the three dimensions (3D) rotor dynamic examination of a material shaft, which allows for an accurate dynamics analysis strategy of the rotor behavior, such as shear stress, torque capacity, and resonance. The static structural, modal analysis, and the harmonic response of the rotor shaft made up of steel, titanium alloy, carbon/epoxy, and boron/epoxy were investigated. The results of the study indicate that boron/epoxy has the highest value of shear stress, torque capacity, and minimum resonance speed point up to 300 Hz. The weight of the carbon/epoxy material is also relatively low when compared to the results of other materials like steel and titanium alloy. Furthermore, the study found that the weight reduction is between 49% to 76% for the boron/epoxy and carbon/epoxy materials compared to a traditional steel shaft. In conclusion, the designed composite shaft, particularly the boron/epoxy and carbon/epoxy materials, has been shown to be the most effective replacement for traditional steel shafts, as they possess superior mechanical properties and result in a significant weight reduction.

Keywords
Rotodynamic, Hollow shaft, Composite materials, Finite element analysis, Critical speed.

1.Introduction
Composite materials have been used more and more over the years, mostly in the aerospace and auto industries. This is because there are so many ways to get the proper properties for different uses. Composite shafts are growing in popularity as a practical solution to the problems present in metallic shafts, and one of the most promising applications is in rotor dynamics [1, 2].

A shaft is a rotating machine component that is responsible for supplying power from the source to the necessary part [3]. Tangential force transmits power to the shaft, and the resulting torque supports it in transmitting power to various elements attached [4, 5]. The clutch assembly transfers power from the engine to the drive shafts, which then send it through the transmission system to the rear wheels, which are ultimately responsible for moving the vehicle.

One of the design engineers' targeted outcomes is improving the automobile's fuel economy. Thorough theoretical and practical study confirms the possible use of composite material in vehicle and helicopter tail rotor shafts [6, 7].

Carbon steels are commonly used in shafts for vehicle applications but are relatively heavier due to their high density [8]. According to the rule of thumb, roughly 22% of the engine's power is wasted because heavier components demand more energy to rotate. In addition, metallic shafts have weight, critical speed, and vibration limits.

Composite materials can be used to replace traditional shaft materials since they have high specific strength and modulus without compromising the component's dependability. Composite materials are made up of two materials that have distinct physical and chemical characteristics. It is lighter and stronger and can provide design flexibility and provide resistance to corrosion as well as wear. Compared to conventional materials, composite

*Author for correspondence

materials also provide a longer fatigue life [9, 10]. By adjusting parameters such as fibre and matrix composition, fibre orientation, number of layers, stacking sequence, layer thickness, and other geometric factors, the stiffness and damping qualities of composite material shafts may be modified. In this way, the rotor system's critical velocities may be easily adjusted to meet the demands of a given project. As the system reaches critical speeds, the vibration amplitudes may also be reduced. Shaft vibration amplitudes at high speeds can be reduced by using composite material, however, this might lead to system instability [11]. Currently, functionally graded materials (FGM) are frequently used to address reliability and durability problems that arise when various materials with different mechanical properties such as variations in hardness, toughness, thermal and residual stresses, and strengths of the interfaces are used within one application.

Depending on the combinations of elements employed, FGMs were first categorized by researchers as standard composite materials. FGMs may be created using a wide variety of material combinations. As indicated in *Figure 1*, the most typical combinations are presented.

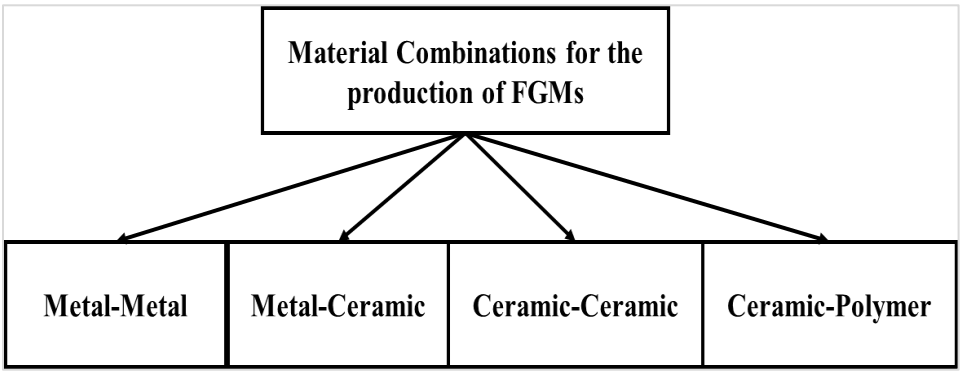

Figure 1 Examples of possible material combinations used in FGMs

The mathematical model of the general physical phenomena is widely used and the simulation considering the most promising tool in the field of material and engineering sciences [12–16]. Composite shafts are often modelled using simplifying assumptions, which allow for a sufficiently realistic representation of the system's dynamic behaviour while keeping a suitably low computing cost. For the study of composites, many new finite element formulations have been presented, including those based on homogeneous beam theory, equivalent layer theory, and the more expensive layer-wise models [17, 18].

The present study is carried out by investigating the rotor dynamic analysis of the hollow shaft at composite materials such that carbon/epoxy and Baron/epoxy and comparing them with a solid shaft made up of steel and titanium alloy of the same outer diameter, also predict the characteristics of composite materials in the automotive sector such that driveshaft. Identifying the relevant design factors, such as shear stress, torque capacity, failure torque and total deformation of a composite drive shaft may be efficiently designed to fulfil the performance expectations. Analysis of vibration characteristics also studied such as critical speed, whirling frequency and natural frequency. The shaft might be solid or hollow circular, but hollow shafts are stronger per kilogram of weight than solid shafts. The stress distribution in a solid shaft is zero in the middle and highest at the outside surface, but the stress distribution in a hollow shaft is smaller, therefore, in this present study, the hollow circular cross-section is chosen. In the current study, engineering simulation software (ANSYS) is used for performing the computational analysis of hollow and solid shaft systems.

The paper was organized into several sections, starting with an introduction in Section 1, followed by a literature review in Section 2. In Section 3, the finite element model was developed to design the hollow shaft for both steel and composite materials. Subsection 3.1 presented the mathematical model related to the dynamic characteristics of the shaft, while subsection 3.2 detailed the material properties of the shaft. The design of the hollow shaft was crucial to the project's success, and both the mathematical model and the material properties played significant roles in this process. Section 4 primarily presented the numerical results of the rotor

dynamics. A rotor dynamic analysis was conducted using the steps outlined in the materials and techniques section, and the results were discussed. The rotor dynamic analysis was a critical component of the project, and the numerical results provided valuable insights into the project's overall performance. Finally, in Section 5, the conclusions and future works remarks were summarized. The future works remarks emphasized the need for further research, particularly in comparing other materials and geometries to gain a better understanding of the mechanical parameters that best suit the project.

2.Literature review

The dynamic analysis of rotating composite shafts was carried out using well-known research [19–21], composite hollow shafts and solid shafts were subjected to both numerical and experimental investigations, with an emphasis on eigenvalues, damping estimates, and imbalance reactions, torque capacity and critical speed [18, 22–24]. These findings prepared the path of employing the composite material for various automobile shafts, centrifugal separators, and marine industrial rotor shaft applications [25, 26] to improve shaft stiffness and move the natural frequency above the operational speeds [27–30]. Also, give designers the option of achieving specified behaviour in terms of critical speed location by rearranging the different composite layers the number of plies and their direction such that [31, 32]. Therefore, in these studies, researchers looked at how changing the orientation of the fibres and the order stacked, in addition, affected the composite drive shaft's first natural frequency and bending torque by constructing a finite element model for a composite drive shaft. Because of spacing constraints, the length and outer radius of drive shafts must be kept to a minimum. Other dimensions like the interior radius, layer thickness, layer number, fibre orientation angle and layer. Stacking sequence are free to be manipulated throughout the design process. These parameters are limited in the best design of the drive shaft by the lateral natural frequency, torsional vibration, and torsional strength.

Investigate how fiber orientation influences composite samples made from natural fibers such as flax, hemp, and kenaf. The composite samples were created using a procedure that combines hand layup with cold compression [33]. A recent study analysed the dynamic instability of a composite shaft that rotates on an internal damper such that [34–36] gave an account of a helicopter's tail rotor driveshaft made of a boron/epoxy composite. Using the equivalent modulus beam and layer-wise beam theories, we analysed how the stacking sequences, fibre orientation, and transversal shear impact affected the natural frequencies and instability thresholds of the shaft. It was shown that the threshold of shaft instability depends on the laminate's characteristics. A damping estimate was provided by Alwan et al. [37].

The ideal design of the drive shafts aims to achieve low values for weight, high values for critical torque, and high values for critical speed. The eigenvalues, damping estimates, and imbalance responses of the rotor system were the primary focus of both numerical and experimental evaluations conducted on composite tube shafts and solid shafts. The mathematical formulation of a rotating shaft with shape memory alloy wires embedded in it was proposed by [38, 39] in these studies the simulations showed how the wire design is related to the rotor system's critical speeds also, all of the composite hollow shaft's anisotropy was considered in the model.

The findings of ANSYS simulations reveal that composite materials are the best materials for designing shafts, signifying the best option for the driving shaft. Because of its great strength and low weight, the automotive design may be optimized, and the vehicle's fuel consumption can be lowered. The present study received special attention, in this study, the effects of varying rotation speeds on the dynamic behaviour of composites including carbon/epoxy and boron/epoxy were examined and compared with steel and titanium alloy materials.

3.Methods

In order to characterise the vibration of the rotor dynamic bearing shaft where torsional stress and modal analysis are performed, it is necessary to assess the material strength related to the power supplied by the shaft. For these purposes, a simulation tool is considered a promising tool considered to this field [40]. Therefore, a finite element analysis tool, engineering simulation software (ANSYS) is utilized for the application of the three dimensions (3D) rotor dynamic examination of composite material.

This study uses mathematical formulation to calculate the performance of the rotor shaft when using both models at two main materials steel and titanium alloy as metallic materials and composite

materials such as carbon/ epoxy and boron/epoxy therefore, a block diagram illustrated in *Figure 2* shows the finite element process used to determine the dynamic response of rotor dynamics of the hollow shaft system.

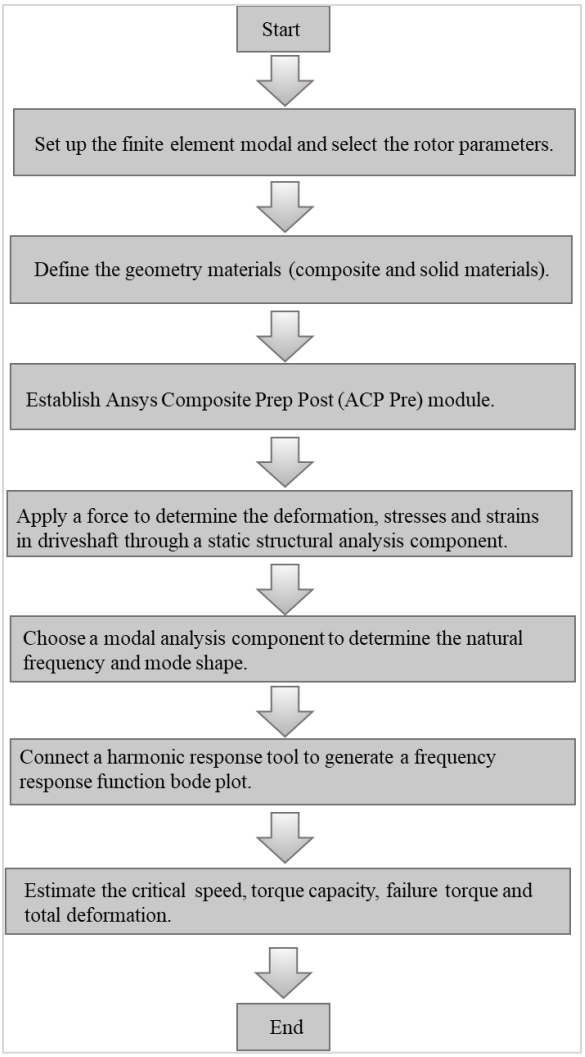

Figure 2 Block diagram for the rotor dynamics approach

3.1Finite element formulation

A composite shaft can be made by wrapping many plies of embedded fibres onto a cylinder, as illustrated in *Figure 3(a).* As can be seen in *Figure 3(b),* each ply exhibits an orthotropic mechanical behaviour. In this case, the orthotropic axes are (1, 2, 3). Hence, 1 represents the fibre direction, 2 is the transverse direction of the fibres in the ply, 3 is the perpendicular direction of the ply, and φ the ply fibre angle.

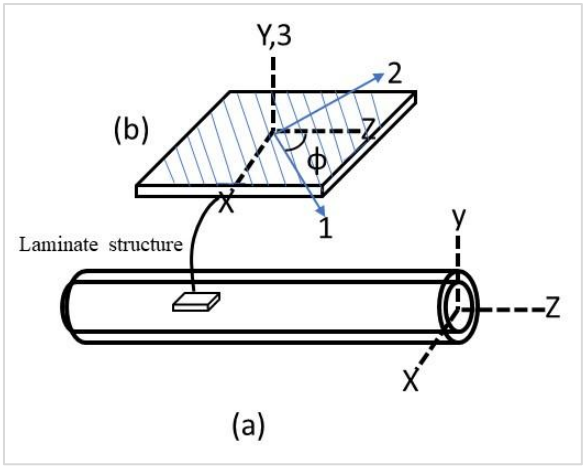

Figure 3 a) Composite rotor b) plan of ply

For an orthotropic material, the generalized Hooke's law is expressed as shown in Equation 1 [23].

$$\{\sigma\} = [Q]\{\epsilon\}, or\ \{\epsilon\} = [S]\{\sigma\} \quad (1)$$

where $\{\sigma\}$ and $\{\epsilon\}$ are the stress and strain stiffness components, $[S]$ and $[Q]$ is the compliance and stiffness matrices respectively, the inverse of the compliance matrix equals the stiffness matrix. The stiffness matrix can be determined by considering that $[Q] = [S]^{-1}$ so only the term of the compliance matrix will be formulated here as shown in Equation 2.

$$\begin{Bmatrix} \epsilon_1 \\ \epsilon_2 \\ \epsilon_3 \\ \gamma_{23} \\ \gamma_{13} \\ \gamma_{12} \end{Bmatrix} = \begin{bmatrix} 1/E_1 & -v_{21}/E_2 & -v_{31}/E_3 & 0 & 0 & 0 \\ -v_{12}/E_1 & 1/E_2 & -v_{31}/E_3 & 0 & 0 & 0 \\ -v_{13}/E_1 & -v_{31}/E_2 & 1/E_3 & 0 & 0 & 0 \\ 0 & 0 & 0 & 1/G_{23} & 0 & 0 \\ 0 & 0 & 0 & 0 & 1/G_{13} & 0 \\ 0 & 0 & 0 & 0 & 0 & 1/G_{12} \end{bmatrix} \begin{Bmatrix} \sigma_1 \\ \sigma_2 \\ \sigma_3 \\ \tau_{23} \\ \tau_{13} \\ \tau_{12} \end{Bmatrix} \quad (2)$$

In this case, the orthotropic axes are (1, 2, 3) as seen also in *Figure 3(b).* Hence, 1 represents the fibre direction, 2 is the transverse direction of the fibres in the ply, 3 is the perpendicular direction of the ply, and φ the ply fibre angle. Each plies plane stress condition may be uniquely identified ($\sigma_{33} = 0$).

After that, the preceding relationship may then be split into the membrane effect and transverse shear effect. as shown in Equation 3.

$$\begin{Bmatrix}\epsilon_1\\ \epsilon_2\\ \gamma_{12}\end{Bmatrix}=\begin{bmatrix}1/E_1 & -v_{21}/E_2 & 0\\ -v_{12}/E_1 & 1/E_2 & 0\\ 0 & 0 & 1/G_{12}\end{bmatrix}\begin{Bmatrix}\sigma_1\\ \sigma_2\\ \tau_{12}\end{Bmatrix} \quad \text{and,}$$

$$\begin{Bmatrix}\gamma_{23}\\ \gamma_{13}\end{Bmatrix}=\begin{bmatrix}1/G_{23} & 0\\ 0 & 1/G_{13}\end{bmatrix}\begin{Bmatrix}\tau_{23}\\ \tau_{13}\end{Bmatrix} \quad (3)$$

For each ply, the following variables must be specified; E_1 and E_2 are young moduli in the orthotropic axes, and G_{23}, G_{13} and G_{12} transversal shear moduli, and v_{12} and v_{21} Poisson's ratios. The shear moduli G_{23} and G_{13} are generally difficult to estimate when thinking about transversal shear effects, thus it is common to practise just assuming they have the same value as G_{12}.

Accordingly, Hooke's law is recalled, and the stress-strain relationships of the angle φ lamina are given as shown in Equation 4.

$$\begin{Bmatrix}\sigma_1\\ \sigma_2\\ \tau_{12}\end{Bmatrix}=\begin{bmatrix}U_1+U_2\cos 2\theta+U_3\cos 4\theta & U_4-U_3\cos 4\theta & \frac{U_2}{2}\sin 2\theta_1+U_3\sin 4\theta\\ U_4-U_3\cos 4\theta & Q_{22}=U_1-U_2\cos\theta+U_3\cos 4\theta & \frac{U_2}{2}\sin 2\theta_1-U_3\sin 4\theta\\ \frac{U_2}{2}\sin 2\theta_1+U_3\sin 4\theta & \frac{U_2}{2}\sin 2\theta_1-U_3\sin 4\theta & \frac{1}{2}(U_1-U_4)-U_3\cos 4\theta\end{bmatrix}\begin{Bmatrix}\epsilon_1\\ \epsilon_2\\ \gamma_{12}\end{Bmatrix} \quad (4)$$

And

$$\begin{Bmatrix}\tau_{23}\\ \tau_{13}\end{Bmatrix}=\begin{bmatrix}G_{23} & 0\\ 0 & G_{13}\end{bmatrix}\begin{Bmatrix}\gamma_{23}\\ \gamma_{13}\end{Bmatrix} \quad (5)$$

Where,

$$U_1=\frac{1}{8}\left(\frac{3E_1}{1-\theta_{12}\theta_{21}}+\frac{3E_2}{1-\theta_{12}\theta_{21}}+\frac{3\theta_{12}E_2}{1-\theta_{12}\theta_{21}}+4G_{12}\right)$$

$$U_2=\frac{1}{2}\left(\frac{E_1}{1-\theta_{12}\theta_{21}}-\frac{E_2}{1-\theta_{12}\theta_{21}}\right)$$

$$U_3=\frac{1}{8}\left(\frac{E_1}{1-\theta_{12}\theta_{21}}+\frac{E_2}{1-\theta_{12}\theta_{21}}-\frac{2\theta_{12}E_2}{1-\theta_{12}\theta_{21}}-4G_{12}\right)$$

$$U_4=\frac{1}{8}\left(\frac{3E_1}{1-\theta_{12}\theta_{21}}+\frac{3E_2}{1-\theta_{12}\theta_{21}}+\ -4G_{12}\right)$$

The general rotor dynamic system as shown in Equation 6.

$$[M]\{\ddot{u}\}+([C]+[G(\Omega)])\{\dot{u}\}+([R]+[K])\{u\}=\{F\} \quad (6)$$

Where $[K]$, $[M]$ are the elastic stiffness matrices and symmetric mass, in addition, $[C]$, $[G]$ are is the global asymmetric damping and antisymmetric gyroscopic matrices (function of the speed of rotation (Ω)) component the external force component, $[R]$ a stiffness matrix as a function of the internal damping of the rotating shaft.

The elemental mass at any layer joining nodes i and j in a normalized coordinate system of x ranging from 1 to -1 is given in Equation 7.

$$[M_e]=\int_{-1}^{1}\int_{-1}^{1}\int_{-1}^{1}[N_i]\rho[N_j]\,dxdydz \quad (7)$$

ρ is the material density, and [N] is the matrix of element shape function for each node at i and j. The elemental stiffness matrix is provided by Equation 8.

$$[K_e]=\int_{-1}^{1}\int_{-1}^{1}\int_{-1}^{1}[B]^T[\bar{D}][B]\,|J|dxdydz \quad (8)$$

where [B] is the strain matrix of the element, [J] is the Jacobian matrix, and $[\bar{D}]$ is the stiffness matrix of the converted material, defined as $[T]^{-1}[D][T]$, [T] is the transformation matrix.

The local coordinate system formulation of the material stiffness matrix [D] is given in Equation 9.

$$[D]=\begin{bmatrix}\frac{E_1}{1-\theta_{12}\theta_{21}} & \frac{E_2\theta_{12}}{1-\theta_{12}\theta_{21}} & 0 & 0 & 0\\ \frac{E_2\theta_{12}}{1-\theta_{12}\theta_{21}} & \frac{E_2}{1-\theta_{12}\theta_{21}} & 0 & 0 & 0\\ 0 & 0 & \kappa G_{12} & 0 & 0\\ 0 & 0 & 0 & \kappa G_{12} & 0\\ 0 & 0 & 0 & 0 & G_{12}\end{bmatrix} \quad (9)$$

The Kelvin-Voigt model is used to represent the isotropic bearing supports, which include stiffness and viscous damping characteristics.

The dynamic response in any mode of vibration of a vibrating system is given as $\{u_i\}=\{\varphi_i\}e^{\lambda_i t}$ e, and the quadratic equation of the Eigen solution is given in Equation 10.

$$-\lambda_i^2[M]_{\{\varphi_i\}}=[K]_{\{\varphi_i\}}+\lambda_i[M]_{\{\varphi_i\}} \quad \text{where} \quad \lambda_i=a_i+jb_i \quad \text{and} \quad \delta_i=2\pi\frac{a_i}{b_i} \quad displacement \quad (10)$$

φ_i is the displacement vector and λ_i is the complex value at the mode i, the real component of the eigenvalue a_i indicates the Eigen problem's stability, b_i are the imaginary eigenvalues indicating damping frequency, The logarithmic decrement δ_i is the ratio between two successive peaks in the dynamic response and the model damping ratio ξ can be calculated as this value.

Finally, the strain energy of each element can be determined as shown in Equation 11.

$$U_e=\frac{1}{2}\sum_{i=1}^{n}\{\sigma\}^T\{\epsilon\}V_i+\frac{1}{2}\left(\{u\}^T\{K_e\}\{u\}\right) \quad (11)$$

Where $\{\sigma\}$ and $\{\epsilon\}$ are the stress and elastic strain components respectively, n is the nodal integer points number, V_i is the volume at each nodal integer i, $\{u\}$ is the degree of freedom component at the element and $\{K_e\}$ is the stiffness matrix of the elements.

However, *Figure 4* shows the distribution of torsional shear stress in a hollow shaft where the value for τ is minimal at r_1 ($d_i/2$) and greatest at r_2 ($d_o/2$) and the shear stress (torque capacity τ_{max}) for a hollow shaft is given in Equation 12.

$$\tau_{max} = \frac{16T \times d_o}{\pi \times (d_o^4 - d_i^4)} \quad (12)$$

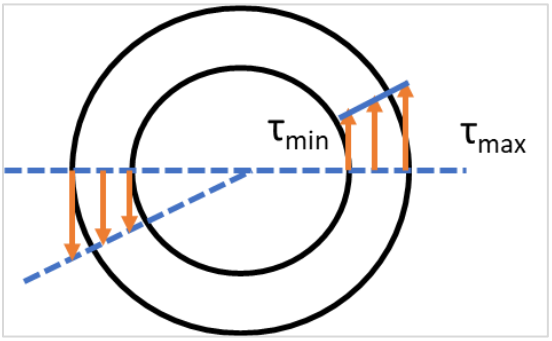

Figure 4 Torsional shear stress distribution

Also, the failure torque is given in Equation 13.

$$\text{Failure torque} = S_{12} \times r^2 \times 2\pi \times t \quad (13)$$

where S_{12} and t are the tensile strength and thickness of the hollow shaft respectively.

3.2Materials

Carbon/epoxy and Boron/epoxy composite material systems are employed and compared with conventional rotating shafts that are manufactured of steel, but titanium alloy is occasionally also utilized, the material properties are given in *Table 1*.

The geometric details of the selected shaft system under investigation included the layer thickness, the number of layers and layer sequences of the composite materials is shown in *Table 2*. The finite element model is also given in *Figure 5*. The thickness of each layer is 1.4 mm, and the fiber orientation is (90, 45, -45,06, 90) (from inner to outer layers). The analysis is performed for 10-ply shafts. The natural frequency may be raised by raising the modulus of elasticity in the longitudinal direction of the shaft, and this is why a zero-degree fibre orientation is so crucial [41].

Table 1 Material properties

	Modulus (GPa)				**Strength (MPa)**				
	Tensile		**Shear**		**Tensile**	**Shear**		**Density (kg/m3**	**Poisson's ratio**
Material	E_1	E_2	G_{12}	G_{23}	S_1	S_{12}	S_{23}	P	υ_{12}
Steel	210	210	84	84	950	450	-	7830	0.3
Carbon/Epoxy	134	7	5.8	5.8	880	97	15	1600	0.3
Titanium Alloy	96	96	35.2	35.2	930	550	-	4620	0.36
Boron/Epoxy	200	19.6	7.5	5.5	1500	110	15	1967	0.3

Table 2 Details of the hollow composite shaft

Specifications	**Length**	**Mean radius**	**Number of layers**	**Layer thickness**	**Fiber orientation angle**	**Isotropic Bearing stiffness**	**Isotropic Bearing damping**
Parameters	1500 mm	31.5mm	10	1.4 mm	[90,45,-45,0_6,90]	5e4 N/mm	1 Ns/mm

The steps to handle the static and dynamic problems in the ANSYS workbench are demonstrated in *Figure 6*. The multilayer composite materials' fiber orientation, model inspection, failure analysis, and parameterization may all be captured with the help of the ANSYS Composite Prep Post (ACP Pre) module. The plies were introduced to the ACP model of Ansys starting with a constant diameter and piled in an outward normal orientation as shown in *Figure 5*. Every ply is described separately, and the program converts this structure into a solid model. This kind of modelling allows for a ply-by-ply investigation of the system's behaviour.

The deformation, stresses, strains, and forces in structures or components induced by loads are determined through a static structural analysis component as shown in *Figure 6*. The natural

frequency and mode shape of a component are determined using modal analysis, which is a dynamic analysis. The mode shape and natural frequency are essential parameters to consider when designing a component for dynamic loading such that critical speeds and system stability.

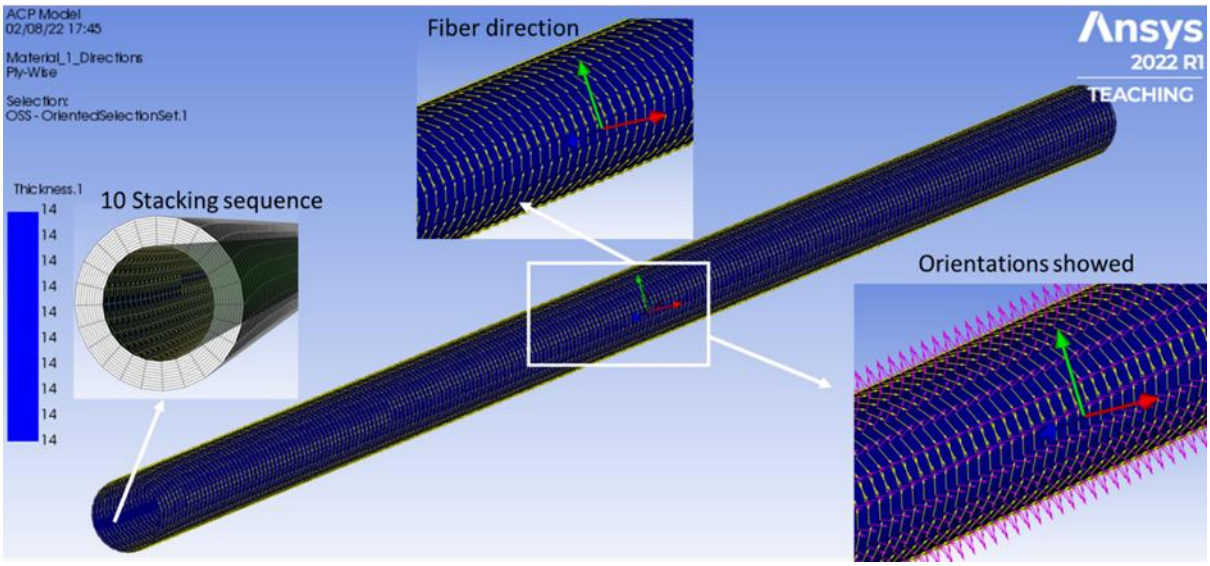

Figure 5 Finite element model of the rotating shaft made from fiber composite materials

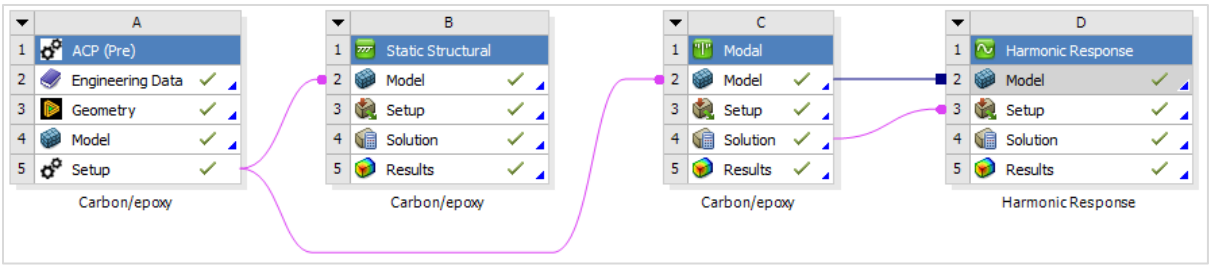

Figure 6 Analysis steps of the composite materials in Ansys workbench

After that, the ANSYS workbench harmonic response tool is connected to generate a frequency response function bode plot.

Two proposed case studies of the hollow shaft are investigated, the shaft with selected materials comprises ten-layered laminated composite rotor shafts with thin walls which are considered fixed at one end and the other end moment is applied as displayed in *Figure 7(a).* The different variants are shown in *Figure 7(b),* where the shaft is held in position by two end bearings. The analysis of the two cases is carried out using ANSYS finite element model.

The strength of the composite shaft under transmitted power is evaluated using torsional stress analysis, as shown in *Figure 7(a),* where the maximum working torque of 3000 Nm is impacted at one end of the shaft while the other end is held constant.

Harmonic analysis (dynamic analysis) is used in high-speed rotor-bearing systems to dynamically analyse shafts made of composite materials. In harmonic analysis, all forces are a function of frequency. The force excitation frequency is the same as the rotor spin speed in synchronous response analysis. The response of a rotor due to mass unbalances is frequently determined using synchronous response analysis. The frequency response function between a node's displacement and a forcing function at a node is determined by both forms of harmonic analysis.

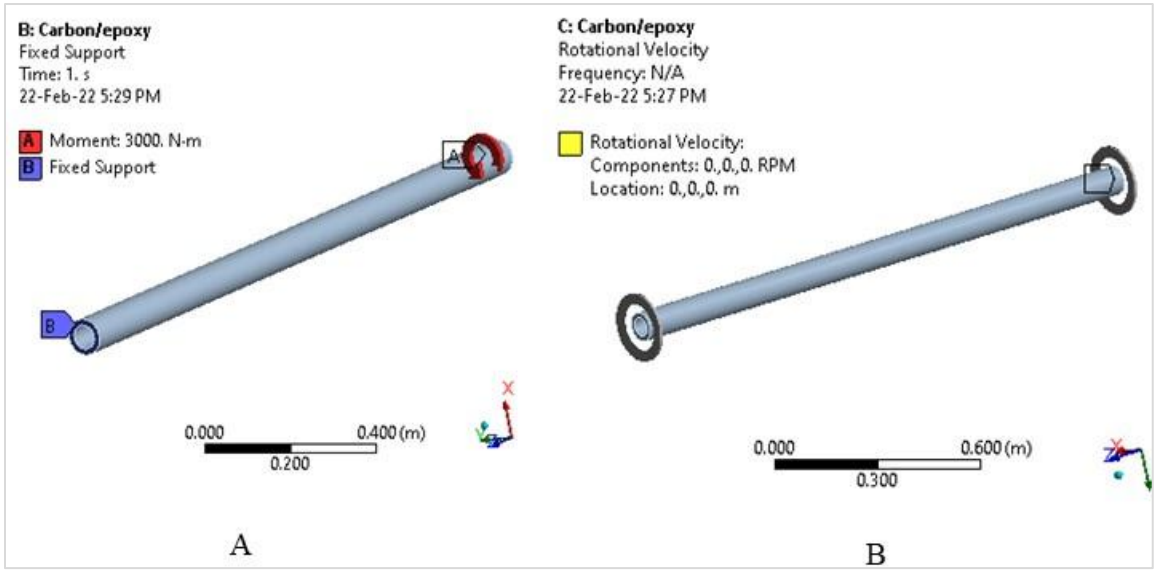

Figure 7 a) Composite driveshaft which fixed end and applied torque at the other end b) hollow shaft supported on two bearing

4.Results

The results of a rotor dynamic analysis conducted by using the steps outlined in the materials and techniques section are shown in the following sections.

4.1Static structure

Figure 8 shows the results of the statics structure analysis performed on four materials; carbon/epoxy composite, steel, titanium alloy and baron/epoxy composite shaft with one end stationary and the other end torqued at a maximum operation of 3000 N.m. The maximum shear stress was acquired on the outer layers of the two composite materials compared with the outer surface of the steel and titanium alloy.

Table 3 lists the maximum shear stress values for the material that is being used. The maximum and minimum stresses on the outer surface of the shaft are induced at carbon fiber of 203.7 MPa and are about 75 MPa at titanium alloy. In addition, the maximum shear stresses at torque 3000 Nm of all proposed materials are 4.9 MPa, 2.9 MPa, 5.2 MPa and 4.9 MPa for steel, carbon/epoxy, titanium alloy and boron/epoxy respectively. This analysis is required to avoid such a failure. The structure will break if the stress levels predicted by this analysis are higher than allowed. Therefore, the torque capacity of the selected material is calculated as shown in *Table 3* to carry the torque without failure which is directly proportional to the shear strength [42] it can be seen that the maximum torque capacity for all materials that be selected is less than the failure limit so that the rotor shaft is safe.

The results of maximum deformation at the drive shaft of specific materials are shown also in *Table 3*. As displaced the maximum deformation occurs in the titanium alloy shaft and it is more than 3 times compared with the steel shaft. In addition, the composite materials exhibited moderate deformation compared with steel and titanium alloy.

Further, the shear strength of Carbon/epoxy and Boron/epoxy are both about 15 MPa, and as the torque capacity is directly proportional to the shear strength according to Equation 12, the torque capacities of the two composite materials are similarly high, at around 1709.8 Nm.

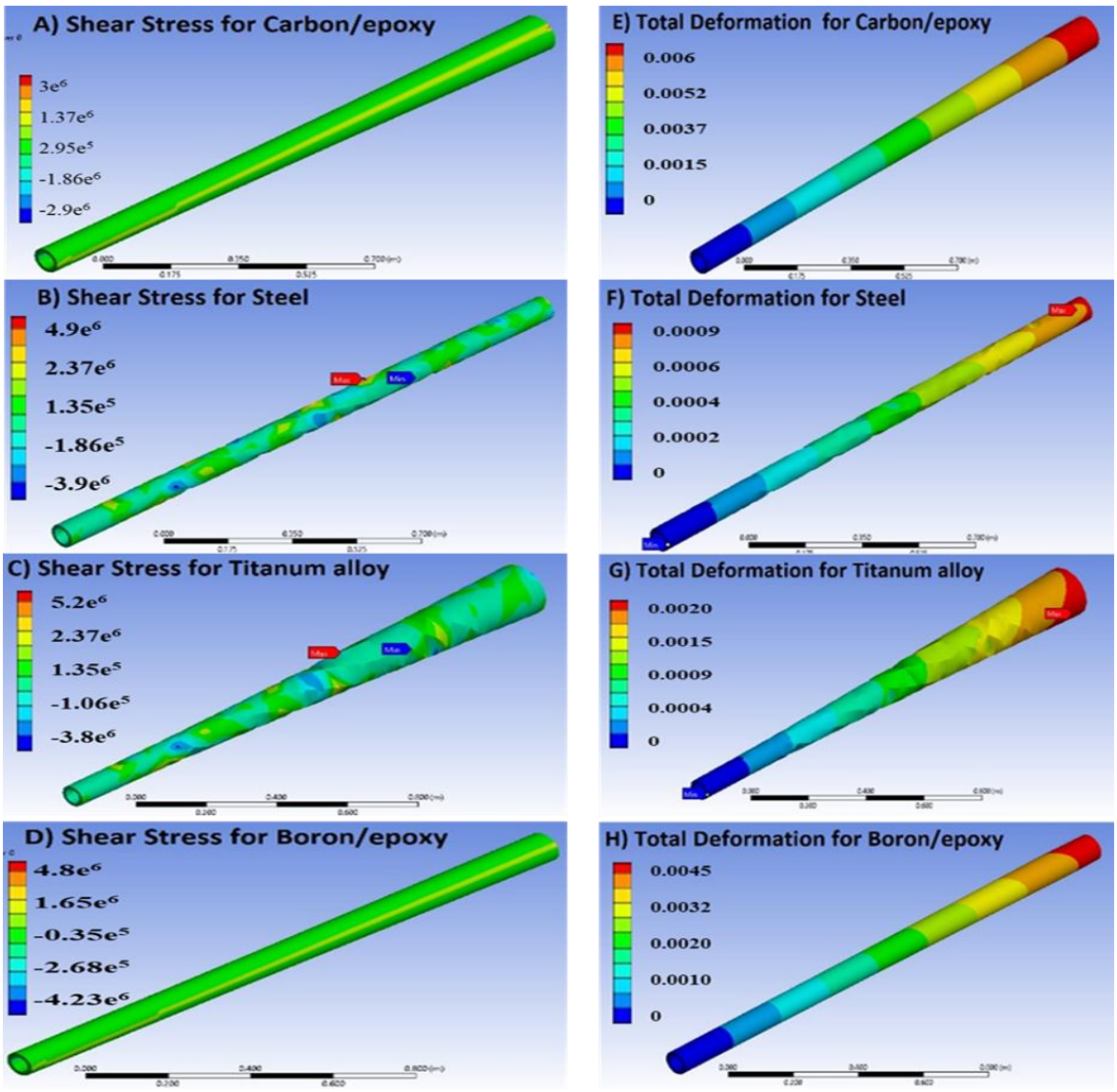

Figure 8 (From A to D) Shear Stress distribution in each material and (from E to H) total deformation at the outer surface of the shaft in each material

Table 3 Static analysis of the hollow shaft at varied materials

Material	Equivalent stress (MPa)	Shear stress (MPa)	Torque capacity (Nm)	Failure torque (Nm)	Total deformation (m)	Weight (Kg)
Steel	83.3	4.9	942.2	39257.3	9.4671e-004	36.22
Carbon/Epoxy	203	2.9	1709.9	6891.9	6.7683e-003	8.856
Titanium Alloy	75.6	5.2	1814.6	47981.2	1.1465e-002	21.22
Boron/Epoxy	94.3	4.9	1709.8	9596.2	1.0687e-003	10.88

Also, as shown in *Table 4*, the results of the modal analysis of the four modes are selected and the critical speed values are determined and evaluated with the conventional steel shaft.

Table 4 Critical speed comparison

BW (Backward whirl) and FW (Forward whirl) while speeding in rpm						
Configuration	Ⅰ BW	Ⅰ FW	Ⅱ BW	Ⅱ FW	Ⅲ BW	Ⅲ FW
Steel	1938.2	1938.8	3784.1	3799.5	9173.4	21832
Carbon/Epoxy	3659.5	3666.2	7740.4	7789.4	15550	33131
Titanium Alloy	2976.2	2981.7	8020.1	8083	18087	34489
Boron/Epoxy	3349.6	3353.1	8819	9115.4	20724	38935

4.2Harmonic analysis

To estimate the rotor-bearing shaft harmonic response, the operation speed is selected to be 30000 rpm (500 Hz) and the magnitude of the displacement vector attributed to the force vector is computed by applying 100 N as an unbalanced force at the end of the rotor's axis of rotation which leads to rotor vibration the amount of vibration due to unbalance force is simulated in ANSYS using frequency response function.

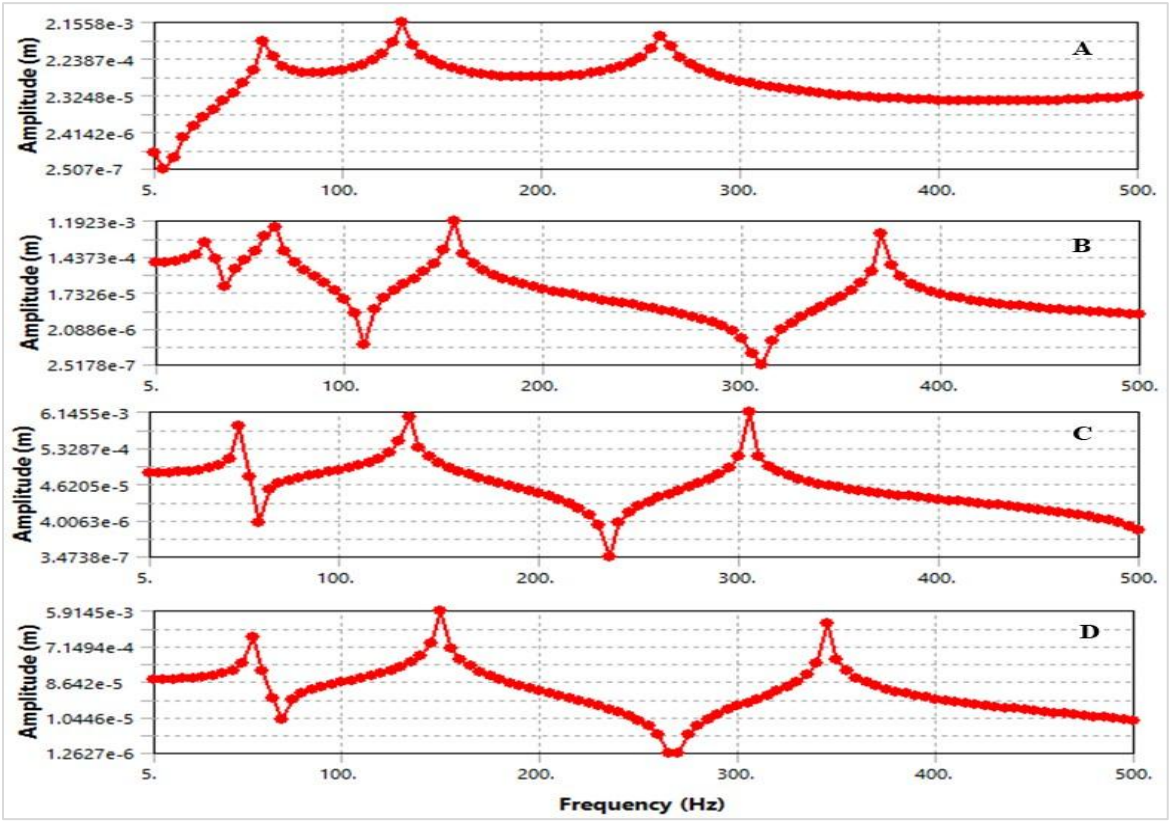

Figure 9 ANSYS frequency response function curve of A) Carbon/epoxy composite, B) Steel, C) Titanium alloy and D) Boron/epoxy composite

Figure 9 illustrates the frequency response function curve of the composite and solid materials shaft up to 500 Hz. As shown the unbalance responses which is the critical speed of the hollow shaft caused firstly at a shaft made of steel at around 50 Hz as seen in *Figure 9(b)* and the instability speeds during the working rotation occur four-time up to 500 Hz in contrary, the instability threshold can be shown just three times on the other materials made from composite materials (*Figures 9(a),9(c)* and *9(d)*), thus, the composite shaft and titanium alloy have less critical speeds than shafts made of other materials throughout the same rotating speed range. Carbon/epoxy shafts do not display a critical speed between 300 and 500 Hz, however, steel shafts show a second critical speed of roughly 70 Hz. When compared to a steel shaft, the critical speed of the composite (carbon and boron epoxy) shaft is much higher under a different state.

5.Discussions

The rotor dynamics of the hollow driveshaft of composite materials (carbon/epoxy and boron/epoxy) are obtained and compared with conventional materials such as steel and titanium alloy by examining two models of hollow shafts, one has an end fixed and the other free to rotate in a bearing, besides, a shaft with two end bearings. *Figure 8* and *Table 3* illustrate how the torsional behaviour of a composite hollow shaft changes significantly while the operating torque remains constant. Static structural analysis for the shaft material shows that three types of material have been identified and behave with stresses plus static deformation compared to other types of materials that have been simulated. The maximum working torque of 3000 Nm shows that the maximum shear stress is 5.2 MPa and 4.9 MPa at the outer surface of the titanium alloy and steel, this means, the conventional materials have more permitted shear stress than composite materials which is required to avoid such a failure. In contrast, the failure torque of the two composite materials is taken place. At 6891.9 Nm and 9596 Nm for Carbon/epoxy and Boron/epoxy respectively, which are more than the failure torque of steel and titanium alloy. In the same manner, the torque capacity limit to transfer torque without exceeding the shaft material's torsional shearing stress of the composite materials at around 1709.8 Nm is higher than the steel and titanium alloy materials. However, the research revealed that comparing composite and steel driving shafts results in a weight reduction of over 79%, while a reduction of around 41% is achieved for that manufactured from titanium alloy for both models with the same length and average radius as shown in *Table 3*.

The results displayed in *Table 3* show that the natural frequencies have been affected by the kind of materials. A shaft made from Carbon/epoxy and Boron epoxy material has a natural frequency that is 52-57 percent higher than that of a traditional steel shaft, making it a superior option. The investigations highlighted that the critical speed of the shaft during the working speed of the Boron/epoxy and Carbon/epoxy is lower than the steel and titanium alloy materials as shown in *Figure 9*. In the end, the overall performance comparisons between the selected material show that the maximum shear stress and torque capacity are found at the driveshaft made from Baron/epoxy composite material, in addition, the minimum number of critical speeds up to 300 Hz is also found at the Baron/epoxy material. Studies on the dynamic behaviour of composite shafts appear to be a crucial topic given the evolving materials utilised in rotating systems (i.e., materials with high performance and low weight). When compared to the identical components built using conventional metallic materials, the adoption of this innovative technology promises to decrease rotating system weight, maintenance costs, noise, and vibration level while increasing efficiency. This study offers the best materials that might be used in the machining process since few studies compare the selected materials that are studied in the research.

However, mechanical characterization of a composite structure is more complex than that of a metallic structure, the design of a fibre reinforced structure is more challenging than that of a metallic structure, mainly due to the difference in properties in directions, the fabrication cost of composites is high, rework and repairing are challenging, and they do not have a high combination of strength and fracture toughness in comparison to metals. A complete list of abbreviations is shown in *Appendix I*.

6.Conclusion and future work

Modern finite element method programs are capable of accurately analyzing rotor behavior to create reliable models and interpret results. In this study, the static structure of carbon/epoxy has the highest value of normal stress resolve and low weight. The boron/epoxy material, on the other hand, has the highest value of shear stress and torque capacity. In addition, the weight of carbon/epoxy is comparable to other materials like steel and titanium alloy.

For modal analysis, composite materials are superior to steel and titanium alloy, with boron/epoxy having a higher critical speed than carbon/epoxy. The harmonic response analysis examines several resonances that occur during the function of shaft rotation, and the simulation results show that boron/epoxy has the fewest number of resonance points when the frequency is 300 Hz. In conclusion, the study recommends using boron/epoxy as the best shaft material due to its advantages in terms of shear stress, torque capacity, critical speed, and the number of resonances points up to 300 Hz. The future work involves a comparison of other materials and geometries to obtain a comprehensive understanding of the mechanical parameters that are most suitable for the project.

Acknowledgment
None.

Conflicts of interest
The authors have no conflicts of interest to declare.

Author's contribution statement
The author confirms sole responsibility for the following: study conception and design, data collection, analysis and interpretation of results, and manuscript preparation.

References
[1] Feroz AA, Chawla D, Kumar R. To study and analyze the design of drive shafts for automobiles using composite material through empirical review on literature. Materials Today: Proceedings. 2022; 56:3820-2.
[2] Chen J, Wang L, Lin J, Tang Y. A pendulum actuator for environmental vibration isolation based on magnetostrictive composite material. Sensors and Actuators Reports. 2022; 4:1-8.
[3] Phadatare HP, Pratiher B. Nonlinear dynamics and chaos of a multi-disk rotating shaft undergoing large deflection mounted on a moving support. International Journal of Non-Linear Mechanics. 2021; 137:1-12.
[4] Yang L, Mao Z, Chen X, Yan R, Xie J, Hu H. Dynamic coupling vibration of rotating shaft–disc–blade system—modeling, mechanism analysis and numerical study. Mechanism and Machine Theory. 2022.
[5] Zhao S, Zhang X, Zhang S, Safaei B, Qin Z, Chu F. A unified modeling approach for rotating flexible shaft-disk systems with general boundary and coupling conditions. International Journal of Mechanical Sciences. 2022.
[6] Vouros S, Goulos I, Pachidis V. Integrated methodology for the prediction of helicopter rotor noise at mission level. Aerospace Science and Technology. 2019; 89:136-49.
[7] Castillo-RS, Tomas-rodriguez M. Helicopter modelling and study of the accelerated rotor. Advances in Engineering Software. 2018; 115:52-65.
[8] Zou D, Zhang J, Ta N, Rao Z. Study on the axial exciting force characteristics of marine propellers considered the effect of the shaft and blade elasticity. Applied Ocean Research. 2019; 89:141-53.
[9] Sivakumar C. Natural frequency and deformation analysis of drive shaft for an automobiles. Materials Today: Proceedings. 2021; 45:7031-42.
[10] Yeswanth IV, Andrews AA. Parametric optimization of composite drive shaft using ANSYS workbench 14.0. International Journal of Mechanical Engineering and Technology. 2018; 8:10-22.
[11] Bucciarelli LL. On the instability of rotating shafts due to internal damping. Journal of Applied Mechanics. 1982; 49(2):425-8.
[12] Goda K, Kajiwara H, Aoyagi M. Examination of hemispherical shell stator for lightweight spherical ultrasonic motor. International Journal of Automation Technology. 2022; 16(4):478-87.
[13] Hara K, Fukuda T, Taguchi K, Isobe H. Surface texturing technique based on ultrasonic turning for improving tribological properties. International Journal of Automation Technology. 2022; 16(1):78-86.
[14] Bhadouria S, Agrawal BN, Singh SK, Nain PK. Study and modal analysis of induction motor by using ANSYS. In advances in mechanical engineering and technology: proceedings of 6th international conference on advanced production and industrial engineering 2021 (pp. 509-19). Singapore: Springer Singapore.
[15] Jain PH, Bhosle SP. Analysis of vibration signals caused by ball bearing defects using time-domain statistical indicators. International Journal of Advanced Technology and Engineering Exploration. 2022; 9(90):700-15.
[16] Shen M, Wang Q, Wang R, Guan X. Vibration analysis of rotating functionally graded graphene platelet reinforced composite shaft-disc system under various boundary conditions. Engineering Analysis with Boundary Elements. 2022; 144:380-98.
[17] Milazzo A. Layer-wise and equivalent single layer models for smart multilayered plates. Composites Part B: Engineering. 2014; 67:62-75.
[18] Arab SB, Rodrigues JD, Bouaziz S, Haddar M. A finite element based on equivalent single layer theory for rotating composite shafts dynamic analysis. Composite Structures. 2017; 178:135-44.
[19] Ala'a M. Examination of the dynamic behaviour of the composite hollow shafts subject to unbalance. International Journal of Mechanical Engineering and Robotics Research. 2021; 10(10):572-6.
[20] Rajak DK, Pagar DD, Kumar R, Pruncu CI. Recent progress of reinforcement materials: a comprehensive overview of composite materials. Journal of Materials Research and Technology. 2019; 8(6):6354-74.
[21] Jamadar IM. A model to estimate synchronous vibration amplitude for detection of unbalance in rotor-bearing system. International Journal of Acoustics & Vibration. 2021; 26(2):161-70.
[22] Hajianmaleki M, Qatu MS. A rigorous beam model for static and vibration analysis of generally laminated composite thick beams and shafts. International Journal of Vehicle Noise and Vibration. 2012; 8(2):166-84.
[23] Sino R, Baranger TN, Chatelet E, Jacquet G. Dynamic analysis of a rotating composite shaft. Composites Science and Technology. 2008; 68(2):337-45.
[24] Barbosa PC, Del CVT, Sousa JMS, Cavalini JAA, Steffen JV. Experimental analysis of the SHBT approach for the dynamic modeling of a composite hollow shaft. Composite Structures. 2020; 236:1-22.
[25] Wang C, Tian J, Zhang FL, Ai YT, Wang Z. Dynamic modeling and simulation analysis of inter-shaft bearing fault of a dual-rotor system. Mechanical Systems and Signal Processing. 2023.
[26] Singh SP, Gupta K. Composite shaft rotordynamic analysis using a layerwise theory. Journal of Sound and Vibration. 1996; 191(5):739-56.

[27] Nadeem SS, Giridhara G, Rangavittal HK. A review on the design and analysis of composite drive shaft. Materials Today: Proceedings. 2018; 5(1):2738-41.
[28] Khoshravan MR, Paykani A. Design of a composite drive shaft and its coupling for automotive application. Journal of Applied Research and Technology. 2012; 10(6):826-34.
[29] Kim CD, Bert CW. Critical speed analysis of laminated composite, hollow drive shafts. Composites Engineering. 1993; 3(7-8):633-43.
[30] Chang MY, Chen JK, Chang CY. A simple spinning laminated composite shaft model. International Journal of Solids and Structures. 2004; 41(3-4):637-62.
[31] Miller B, Ziemiański L. Optimization of dynamic behavior of thin-walled laminated cylindrical shells by genetic algorithms and deep neural networks supported by modal shape identification. Advances in Engineering Software. 2020; 147:1-20.
[32] Badie MA, Mahdi E, Hamouda AM. An investigation into hybrid carbon/glass fiber reinforced epoxy composite automotive drive shaft. Materials & Design. 2011; 32(3):1485-500.
[33] Ramam RS, Padal KT. Effect of fiber orientation on the mechanical properties of natural fiber epoxy reinforced composites of flax, hemp, and kenaf. International Journal of Advanced Technology and Engineering Exploration. 2022; 9(86):72-81.
[34] Bavi R, Hajnayeb A, Sedighi HM, Shishesaz M. Simultaneous resonance and stability analysis of unbalanced asymmetric thin-walled composite shafts. International Journal of Mechanical Sciences. 2022.
[35] Kim K, Ri K, Yun C, Jong Y, Han P. Nonlinear forced vibration and stability analysis of nonlinear systems combining the IHB method and the AFT method. Computers & Structures. 2022.
[36] Li HN, Fu X, Li YL, Liu HJ. Mechanical model and structural control performance of a new rotation-magnified viscoelastic damper. Engineering Structures. 2022.
[37] Alwan V, Gupta A, Sekhar AS, Velmurugan R. Dynamic analysis of shafts of composite materials. Journal of Reinforced Plastics and Composites. 2010; 29(22):3364-79.
[38] Lopatin AV, Morozov EV, Kazantsev ZA, Berdnikova NA. Deployment analysis of a composite thin-walled toroidal rim with elastic hinges: application to an umbrella-type reflector of spacecraft antenna. Composite Structures. 2023.
[39] Udatha P, Sekhar AS, Velmurugan R. Eigen value analysis of composite hollow shafts using modified EMBT formulation considering the shear deformation along the thickness direction. Defence Technology. 2023:1-12.
[40] Cutolo A, Carotenuto AR, Palumbo S, Esposito L, Minutolo V, Fraldi M, et al. Stacking sequences in composite laminates through design optimization. Meccanica. 2021; 56:1555-74.
[41] Rangaswamy T, Vijayrangan S. Optimal sizing and stacking sequence of composite drive shafts. Materials Science. 2005; 11(2):133-9.
[42] Al-falahat M. Implementation of the dynamic balancing approach of a rotating composite hollow shaft. EUREKA: Physics and Engineering. 2022:68-73.

Ala'a Al-Falahat obtained a B.S. degree in Mechanical Engineering from Mutah University, Jordan, in 2007. He pursued an M.S. in Mechanical Engineering from Jordan University, Jordan, and a PhD degree in Mechanical Engineering from the Technical University of Berlin, Germany, which he completed in 2019. Since then, he has been working as an Assistant Professor in the Department of Mechanical Engineering at Mutah University in Jordan. His research interests are focused on Material Science and Dynamic Analysis, including Vibration Control.
Email: alaa.falahat@mutah.edu.jo

Appendix I

S. No.	Abbreviation	Description
1	ACP pre	Ansys Composite Prep Post
2	λ_i	Complex Value At The Mode i
3	$[S]$	Compliance Matrix
4	λ_i	Complex Value At The Mode i
5	ξ	Damping Ratio
6	φ_i	Displacement Vector
7	a_i	Eigenvalue
8	ANSYS	Engineering Simulation Software
9	FGM	Functionally Graded Materials
10	$[G]$	Global Antisymmetric Gyroscopic
11	$[C]$	Global Asymmetric Damping
12	b_i	Imiginary Eigen Value
13	[J]	Jacobian Matrix
14	$[M]$	Mass Matrix
15	ρ	Material Density
16	φ	Ply Fibre Angle
17	Ω	Rotational Speed
18	σ	Stress Stiffness Component
19	ϵ	Strain Stiffness Component
20	$[Q]$	Stiffness Matrix
21	S_{12}	Tensile Strength
22	[T]	Transformation Matrix
23	G	Transversal Shear Moduli
24	t	Thickness
25	3D	Three Dimensional
26	E	Young Moduli